AADE-12-FTCE-50

Drilling Unconventional Shales with Innovative Water-Based Mud – Part I: Evaluation of Nanoparticles as a Physical Shale Inhibitor

Lujun Ji, Quan Guo and Jim Friedheim, M-I SWACO; Rui Zhang*, Martin Chenevert and Mukul Sharma, University of Texas at Austin

Abstract

Although key shales vary considerably in terms of reservoir pressure, temperature, mineralogy and local stresses, the principal drilling-related issues are wellbore stability, shale inhibition, hole cleaning and rate of penetration. Because most of the shale reservoirs are in environmentally sensitive and/or densely populated areas, stricter environmental regulations require new types of environment-friendly water-based drilling fluids. The traditional shale inhibition method through either chemical inhibition or invert emulsions will not be enough to satisfy the increasingly stricter environmental requirement.

This paper focuses on the technique and the performance results of nanoparticles as a physical shale inhibitor by plugging the pores and micro-cracks in shale and preventing water invasion into the shale. The companion paper (Part II) presents the formulations and performance tests of this novel water-based drilling fluid. Pressure and water penetration tests were performed to evaluate water invasion rates into various shale core samples, with initial brine permeabilities varying from less than 1 to over 100,000 nD, due to microfractures. Permeability reduction was used as a proxy of water invasion reduction into shale and thus the effectiveness in plugging pores and microfractures in shale by the nanoparticles. Many orders of permeability reduction were consistently observed for drilling fluids with nanoparticles.

Test results showed that although nanoparticles alone may be effective in preventing water invasion into shale samples with no microcracks, the combination of properly formulated mud and nanoparticles of appropriate material, size and concentration is the key to preventing water flow into shale play core samples with or without microcracks. This new water-based drilling fluid with nanoparticles provides an entirely different type of shale inhibition by physically plugging the shale micro-cracks and pores while meeting the strictest environmental regulations for shale play drilling.

Introduction

Depletion of many conventional oil and gas reserves and increasing demand for energy has increased the importance of shale and techniques to drill shale. While shale has been traditionally considered as hydrocarbon source and/or seal rocks, and shale plays are now recognized as major hydrocarbon reservoir rocks. These unconventional hydrocarbon resources including gas and oil shale have blossomed in recent years. For example, worldwide, likely recoverable shale gas reserves exceed 250 Tcf by some estimates, with over 10 times that speculated to be in place.[1] In North America, shale gas has been one of the most rapidly expanding trends in onshore domestic natural gas exploration and exploitation.

Different from traditionally reactive shales, gas shales are organic-rich, and predominantly comprised of consolidated clay-sized particles, nanopores and natural fractures. The principal drilling-related issues are wellbore stability, shale inhibition, hole cleaning and rate of penetration. The mineralogy and petrophysical characteristics of these shale plays require high quality and cost-effective drilling fluids for successful development of the resources.

Currently, chemical shale inhibitors are used in both oil-based and water-based drilling fluids, or “mud” as it is commonly known, to keep the wellbore stable during drilling operations. Oil-based mud (OBM) is used more often than water-based mud (WBM) in shale gas drilling[2] because most water-based drilling fluids can have profound effects on clay/shale stability. Shale inhibitors are required to minimize the clay/shale interaction, otherwise water in the WBM can diffuse into the shale matrix and cause swelling, delaminating, fracturing of clays and partial solubilization of calcium carbonate, aluminum salts, and other minerals contained in the shale.

Increasingly stricter environmental regulations will require more environment-friendly water-based drilling fluids, shale inhibitors and other workover fluids, especially in environmentally sensitive regions. Freshwater is already a choice over salt water for land operations to control the chloride content.

The material selected for this study is nanosilica. These nanoparticles are potential non-reactive shale inhibitors to physically plug nano-size pores to reduce water invasion, thus reducing shale swelling, and maintaining shale stability. Pressure penetration tests or shale membrane tests have been performed to evaluate the performance of these nanoparticles in water-based drilling fluids and study the impact of the

*Now with China University of Petroleum

drilling fluid with nanoparticles on water activity and shale stability.

This paper, Part I of "Drilling Unconventional Shales with Innovative Water-Based Mud", focuses on the evaluation techniques and the performance test results of nanoparticles as a physical shale inhibitor by plugging the pores and micro-cracks in shale and preventing water invasion into the shale. The companion paper, Part II, presents the mud formulations and performance tests of the novel water-based drilling fluid with nanosilica (nano-WBM).[3]

Evaluation Methodology

Flow-Through Test for Shale Permeability

A transient-flow test (also known as the shale membrane efficiency test or pressure penetration test) was used to measure the impact of physical plugging by nanoparticles on shale permeability using the device shown in Figure 1.[4] The test apparatus consists of a main cell, a pumping system, a back pressure regulation system and a bottom system. A shale sample is installed inside the main cell. Brine, mud or other testing fluid is pumped from the left port into the cell and flows along the top surface of the shale sample and through the right port out of the cell into a waste collection system. The mud flow is maintained at a constant pressure with a back pressure regulator system with nitrogen tank. The bottom system has a tiny volume.

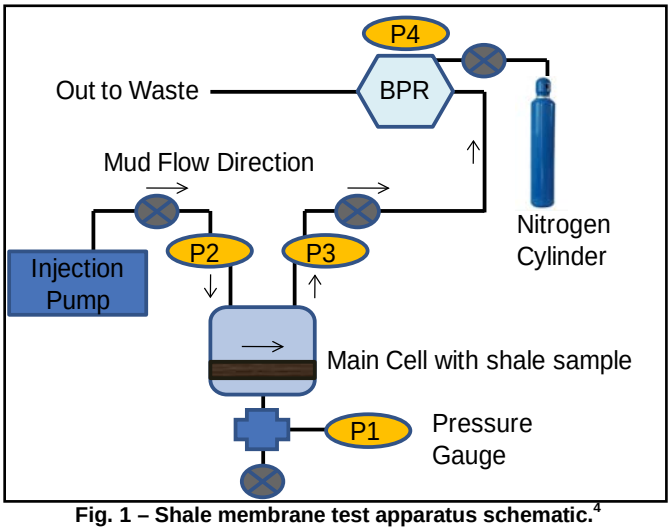

Fig. 1 – Shale membrane test apparatus schematic.[4]

During the test, the test fluid is forced at constant top driving pressure (P2, P3) to flow across a thin shale sample while measuring the increased bottom pressure (P1) in the bottom reservoir. The impact of shale permeability for the test fluid can be interpreted from change in bottom pressure (P1).

Permeability changes (as measured by lack of pressure transmission to the bottom of the test cell) with respect to various test fluids using the same shale sample, are treated as an indicators of physical plugging by solids and nanoparticles particles in the WBM. The more significant the permeability reduction between the WBM and initial brine, the better the physical plugging by the solids and nanoparticles and the more stable the shale is to exposure to the drilling fluid.

We used van Oort's transient pressure model[5] for bottom pressure (P1) variation with time with a known initial condition, homogeneous initial pressure P_0 in the shale and inside the bottom reservoir, and the known constant top driving pressure (boundary condition) P2 at the entry end of a shale sample.

$$\ln\left[\frac{P2-P1}{P2-P0}\right] = -\frac{Ak}{\mu CVL}t \qquad \text{(Eq. 1)}$$

where:

k	=	*permeability of the shale*
t	=	*test time*
A	=	*cross-section area of shale sample*
C	=	*compressibility of fluid in bottom reservoir*
L	=	*thickness of shale sample*
$P0$	=	*initial fluid (pore) pressure in shale sample*
$P2, P3$	=	*top driving pressures above shale sample, flow-in and flow-out, respectively*
$P1$	=	*bottom pressure in reservoir*
V	=	*bottom reservoir volume*
M	=	*fluid filtration viscosity*

The dimensionless bottom pressure is a linear relationship with time t on a semi-log plot, as shown in Figure 2.

Knowing apparatus constants (A, L and V) and fluid properties (C and μ) in Equation (Eq. 2), shale permeability is calculated from the slope of the linear part in Figure 2.

$$k = \left(-\frac{\mu CVL}{A}\right)m \qquad \text{(Eq. 2)}$$

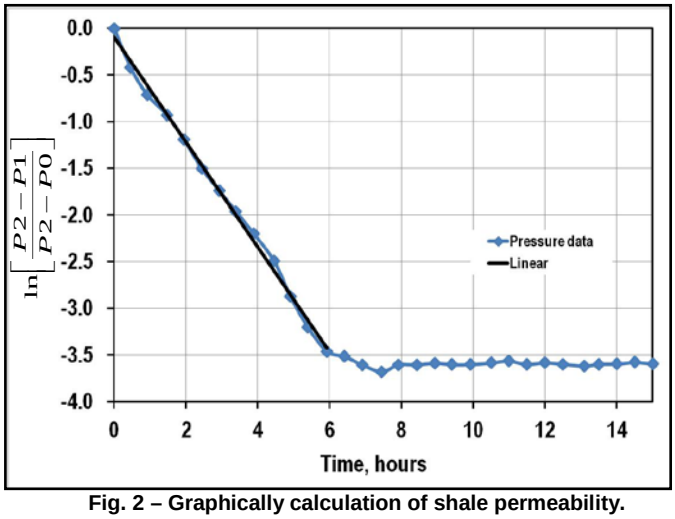

Fig. 2 – Graphically calculation of shale permeability.

Test Procedure to Evaluate Nanoparticles

Generally, the shale membrane test includes at least two steps, using brine and the testing fluid (mud with or without nano-particles), respectively.

Step 1 – Conduct test with 4% NaCl brine. This permeability is treated as a reference.

Step 2 – Test the same shale sample with the testing fluid with or without nanoparticles.

Step 3 – Test with 4% NaCl brine to evaluate the effect on physical plugging with nanoparticles in Step 2.

Reduction between the two permeabilities with respect to various test fluids (brine, mud with/without nanoparticles) is used as a measure of reduction in the water invasion into the shale and thus measuring the effectiveness of plugging the pores and microfractures by the nanoparticles. The more permeability reduction, the better the physical plugging with nanoparticles and the less water invasion, and subsequently, the more stable the shale.

Lab Evaluation of Nanoparticles as a Physical Shale Inhibitor

Tests were run with the brines, a nanoparticle dispersion, and WBM with and without nanoparticles on two types of shale – Mancos shale and a gas shale.

Nanoparticles

The nanoparticles discussed in this paper are uniform 20-nm diameter silica spheres (Figure 3). They have excellent ion compatibility, temperature stability, and no adverse effect on mud properties. More details on the nanoparticles are given in the companion paper.[3]

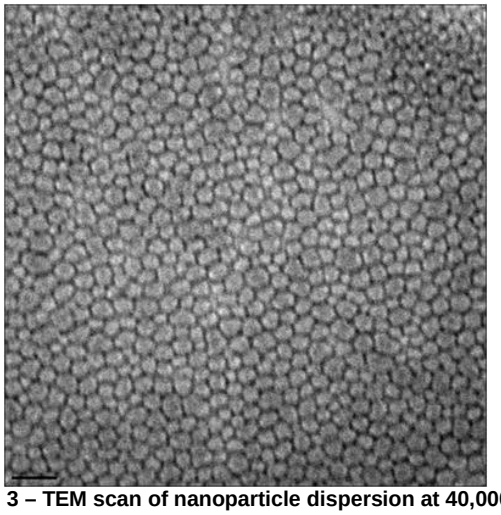

Fig. 3 – TEM scan of nanoparticle dispersion at 40,000× magnification; scale bar (lower left corner) is 50 nm in length.

WBM

A freshwater WBM was used for testing. Details on the novel fresh water-based mud are given in the companion paper[3]. The rheological properties are shown in Table 1.

Mud A is the base mud without any nanoparticles. Mud B and Mud C are made from Mud A. Nano-particle concentration in Mud C is one third of that in Mud B.

Table 1 – WBM Properties

		Fluid		
		A	B	C
Nanoparticle Dispersion	unit		3	1
Density	lb/gal	11.99	11.86	11.95
Rheology				
10-sec Gel Strength	lb/100 ft^2	7	6	5
10-min Gel Strength	lb/100 ft^2	10	8	7
Plastic Viscosity	cP	19	28	28
Yield Point	lb/100 ft^2	36	18	12
pH		9.65	8.7	9
API Filtration	mL	2.4	2.2	2.2
API 100-nm filter	mL	3.0	2.4	2.9
HTHP Filtration				
Temperature	°F		250	
HTHP Filtration (30 min)	mL	13.6	8.8	11.2

Lab Evaluation on Mancos Shale

Mancos shale is medium reactive shale without cracks. Mancos shale contains 18% smectite, including illite/smectite mixed layers and its CEC is 14 meq/100 g. Table 2 lists the Mancos shale mineralogy. Brine permeability of the tested Mancos shale samples was less than 1.0 nD.

Table 2 – Mineralogy of Mancos Shale

Smectite* (%)	18
Illite (%)	5
Calcite (%)	5
Quartz (%)	60
Dolomite (%)	7
Fieldspars (%)	3
Pyrite (%)	1
Kaolinite (%)	1
CEC (meq/100 g)	14
*Includes illite/mixed layers	

Test Set #1 with Brines and Pure Nanoparticle Dispersion on Mancos Shale

Instead of the usually 3-step test, this test set was run with 4 steps – 3 steps with 4% NaCl brine, and then a step with pure nanoparticle dispersion in order to stabilize shale with brine and get shale brine permeability as a reference. The bottom pressures of all 4 steps are plotted in Figure 4 and the corresponding permeability from the pressure curves are listed in Table 3.

Table 3 – Permeability with Brines and Pure Nanoparticle Dispersion on Mancos Shale

Step	Test Fluid	Permeability (nD)
1	NaCl Brine	0.247
2	NaCl Brine	0.191
3	NaCl Brine	0.180
4	Pure nanoparticle dispersion	0.008

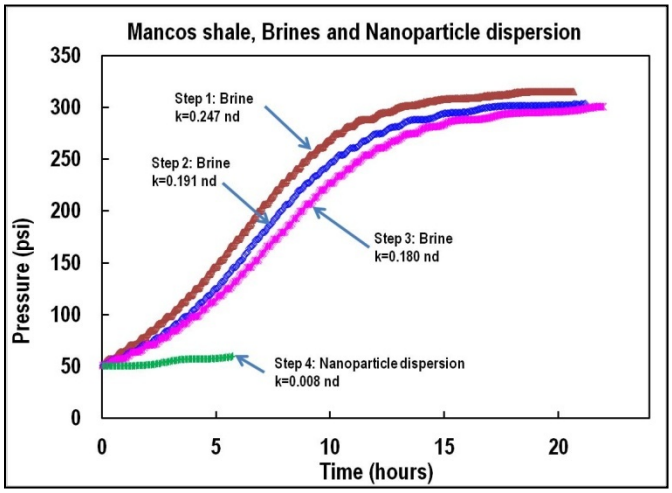

Fig. 4 – Results of shale membrane tests with brines and pure nanoparticle dispersion on Mancos shale.

In the first 3 steps with brine, the bottom pressure builds up more and more slowly, and the brine permeability gradually decreases a little bit after each step due to brine/shale interaction. The shale permeability in the first 3 steps with brine is still in same order of magnitude, and permeability reduction between two consecutive steps is small, compared to the huge permeability reduction in Step 4 with the pure nanoparticle dispersion. The shale permeability with the nanoparticle dispersion (Step 4) is only 0.008 nD, a reduction of nearly two orders of magnitude from 0.180 nD in Step 3 with brine. The nanoparticles nearly shut off water invasion into the shale in this test. This test verifies that the permeability reduction in Step 4 with nanoparticle dispersion is dominantly controlled by physically plugging the shale pores with nanoparticles even though brine/shale interaction causes some degree of shale inhibition and permeability reduction.

Test Set #2 comparing WBM and nano-WBM on Mancos Shale

A 2-step test was performed on Mancos shale with brine and Mud A, the base mud containing no nanoparticles. In this test, the sample was tested first with NaCl brine (Step 1), relaxed for overnight and then tested again with Mud A (Step 2). Figure 5 shows the bottom pressure buildups over time with brine and Mud A.

It is clear that pressure in the bottom reservoir builds up more quickly with brine (red line) than that with Mud A (green line) as the same constant top pressure (300 psi) drives the fluids flowing along the shale sample surface. The increased bottom pressure means that the shale sample was more permeable with brine than with Mud A. The permeability was reduced from 0.5 nD with brine to 0.035 nD with Mud A.

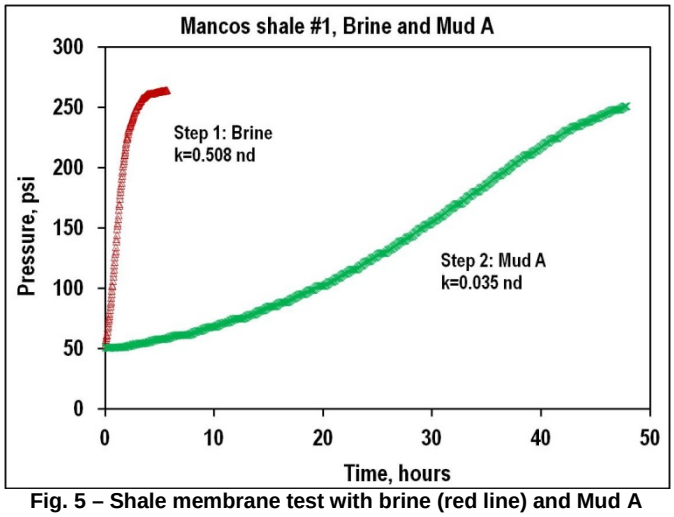

Fig. 5 – Shale membrane test with brine (red line) and Mud A (green line) on Mancos shale Sample #1. Mud A contains no nanoparticles.

Another 3-step test was conducted with Step 1 – brine, Step 2 – Mud C (nano-WBM) and Step 3 – brine again on Mancos shale #2 (Figure 6). Initial permeability of this sample was 0.153 nD with brine (Step 1) and was reduced to 0.0042 nD with Mud C (Step 2). Permeability was significantly reduced, confirming again that the pores in the shale are physically plugged by the nanoparticles in the mud. In other words, water invasion into the shale was significantly reduced due to the physical plugging. An additional step of brine (Step 3) was repeated after Mud C in order to confirm the sustainability of the physical plugging. As shown in Figure 6, the Step 3 pressure (bottom red line) with the same brine overlaps the green curve of Step 2 (Mud C). This confirms that the nanoparticle physical plugging is sustainable.

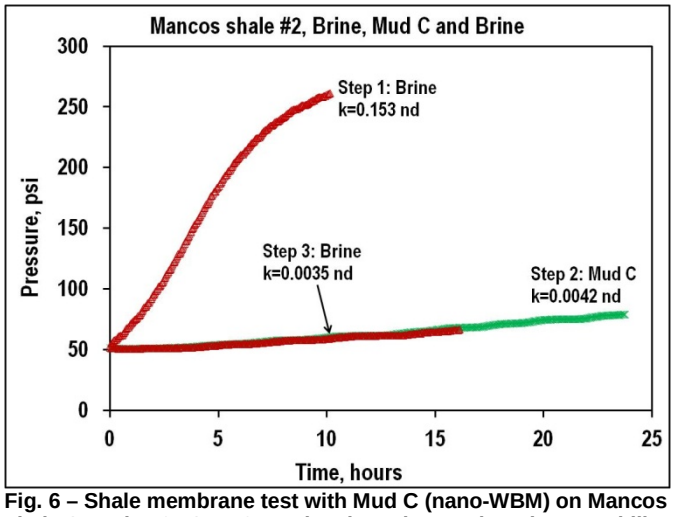

Fig. 6 – Shale membrane test with Mud C (nano-WBM) on Mancos shale Sample #2. Step 3 results show the continued permeability reduction from the nanoparticles.

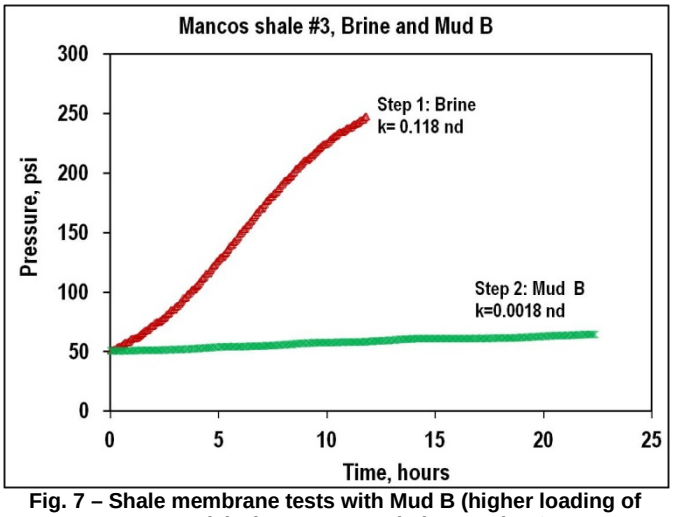

Fig. 7 – Shale membrane tests with Mud B (higher loading of nanoparticles) on Mancos shale sample #3.

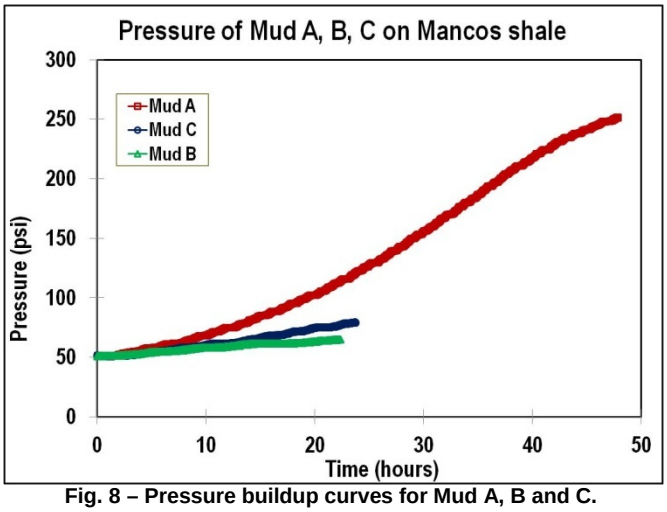

Fig. 8 – Pressure buildup curves for Mud A, B and C. Muds B and C contain nanoparticles.

The third shale membrane test was conducted with Mud B (nano-WBM) on Mancos shale #4 (Figure 7). This test was similar to the second test, but Mud B contains 3 times as much as nanoparticles than Mud C.

In this test, the shale permeability was reduced from an initial permeability of 0.118 nD with brine to 0.0018 nD with Mud B – nearly 99% reduction in permeability. Over 24 hours, the pressure in the bottom reservoir showed only a very slight build up. The nanoparticles in Mud B nearly shut off all water invasion into the shale.

Pressure buildup with Mud A, B and C on these Mancos shale samples are plotted together in Figure 8. It clearly shows that the muds containing nanoparticles (Muds B and C) significantly slowed the pressure build up and indicates a reduction in water invasion by physically plugging the shale pores as compared to the base mud without nanoparticles (Mud A). The higher the nanoparticle concentration, the better plugging, as shown in comparing Mud B and Mud C (Table 5). Permeability with nano-WBM (Muds B and C) was reduced by nearly 2 orders of magnitude. This confirms that nanoparticles do behave as excellent shale inhibitor to Mancos shale by physically plugging the shale pores with nano-particles.

Table 4 – Permeability Reduction with Nanoparticles on Mancos Shale

Test Fluid	Brine Permeability (nD)	Mud Permeability (nD)	Permeability Reduction (%)
Mud A	0.506	0.035	94
Mud B	0.118	0.0018	98
Mud C	0.153	0.0042	97

Table 5 –Mineralogy of Gas Shale

Smectite* (%)	4
Illite (%)	10
Calcite (%)	62
Quartz (%)	21
Pyrite (%)	2
Siderite (%)	1
CEC (meq/100 g)	3
*Includes illite/mixed layers	

Lab Evaluation on Gas Shale

The gas shale mineralogy is shown in Table 5. It is a low reactive shale; CEC is 3 meq/100 g, and contains 4% smectite.

Gas shale sample #1 was naturally fractured. As shown in Figure 9, there exists a crack 50 micron wide across the shale sample. These existing cracks on the gas shale result in a high initial permeability with NaCl brine, over 100,000 nD. Due to the high permeability, normal pressure penetration test can't be run on these gas shale samples because the bottom pressure builds up in couple of minutes to the top driving pressure. Therefore, a steady state flow test was run with brine on these samples for the initial or reference permeability.

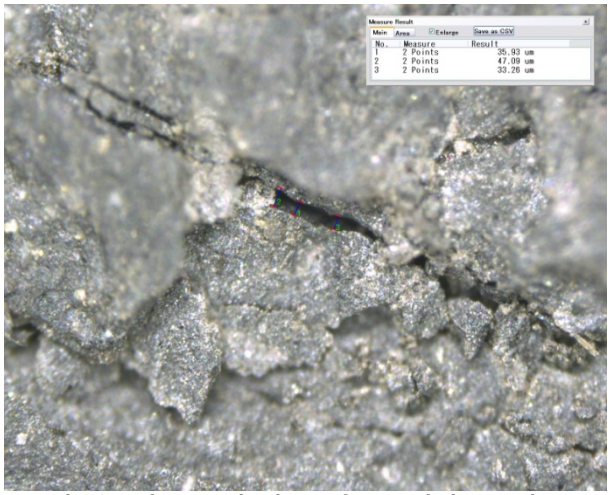

Fig. 9 – Microscopic photo of a gas shale sample.

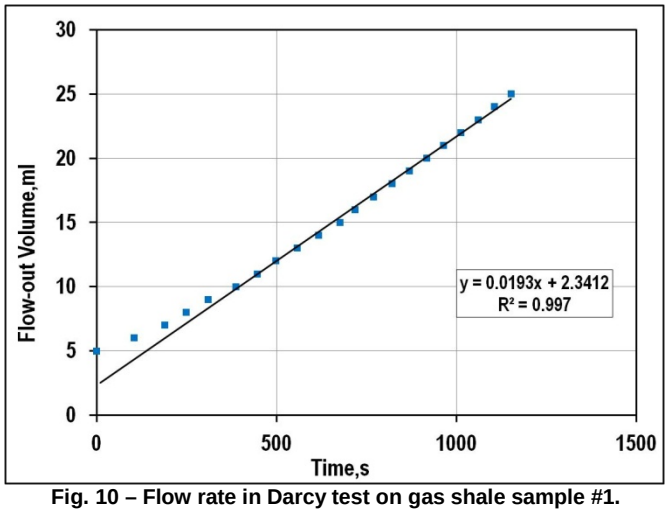

Fig. 10 – Flow rate in Darcy test on gas shale sample #1.

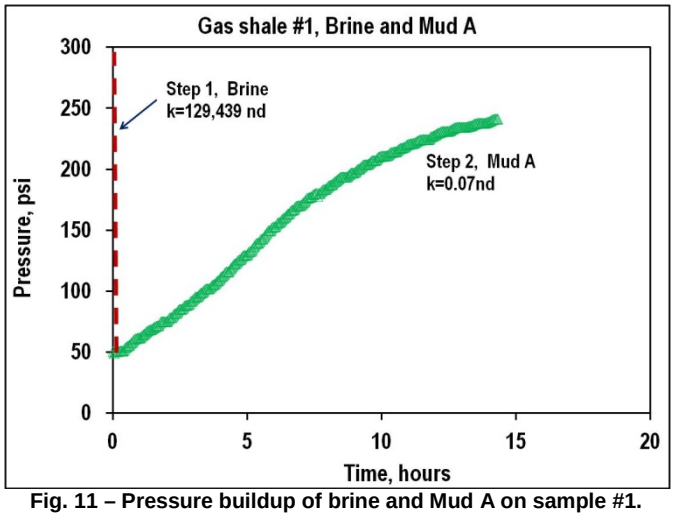

Fig. 11 – Pressure buildup of brine and Mud A on sample #1.

Tests on Highly Fractured Gas Shale

Figure 10 shows a Darcy flow tests for the initial permeability (Step 1) of highly fractured gas shale sample #1.

From the measured fluid (brine) volume flowing across the 0.25-in. thick sample under constant 109-psi pressure differential, the Darcy's flow rate across the sample is linear fitted as 0.0193 mL/s (Figure 10). With shale sample dimension parameters and brine properties in Table 6, this sample has a high permeability, 129,439 nD, due to the existing microcracks.

For the highly fractured gas shale sample discussed in this paper, Step 1 with brine was run with Darcy's steady state flow test, and is schematically illustrated with a dashed red line in Figure 11 and Figure 12 for comparison.

Table 6 – Darcy's Flow Test on Gas Shale Sample #1

Item	Unit	Value
Pressure differential	psi	109
Sample Thickness	in.	0.25
Core cross-section area	cm^2	12.95
Brine viscosity	mPa•s	1
Flow rate	mL/s	0.0193
Permeability	nD	129,439

Figure 11 and Figure 12 show bottom pressure buildup with Mud A and Mud B on the highly fractured gas shale samples.

In Figure 11, the permeability was significantly reduced from the initial 129,440 nD with brine down to 0.07 nD with Mud A as the existing cracks are plugged with mud.

In Figure 12, with Mud B containing nanoparticles, the permeability was significantly reduced from initial 140,049 nD (Step 1 with brine) down to 0.004 nD with Mud C (Step 2). Mud B, with a greater nanoparticle loading, showed a significantly greater reduction in permeability as compared to Mud B.

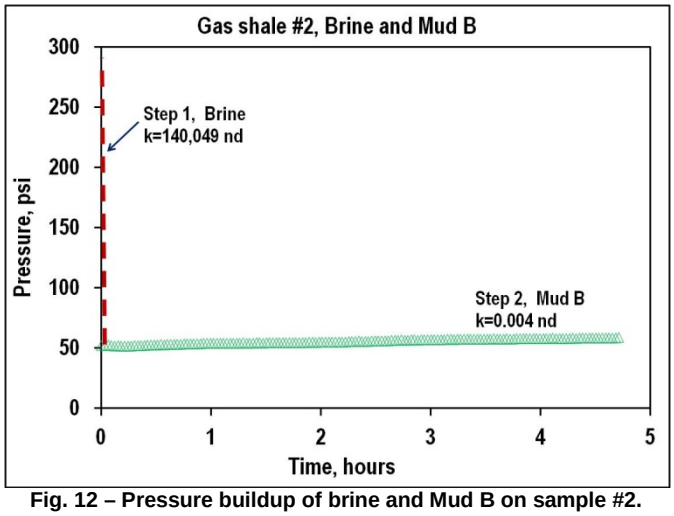

Fig. 12 – Pressure buildup of brine and Mud B on sample #2.

Table 7 – Permeability Reduction on Highly Fractured Gas Shale Sample

Test Fluid	Brine Permeability (nD)	Mud Permeability (nD)	Permeability Reduction (%)
Mud A	129,439	0.07	100
Mud B	140,049	0.004	100

As shown in Figure 13 and Table 7, compared to the high initial permeability (over 100,000 nD) of these highly fractured gas shale samples, the final permeability in both 2 mud cases is small and permeability reduction is very significant, nearly 6 orders of magnitude. That proves that nanoparticles in the novel mud can physically plug both existing cracks and pores in shale and effectively shut off water invasion into shale to maintain shale stability.

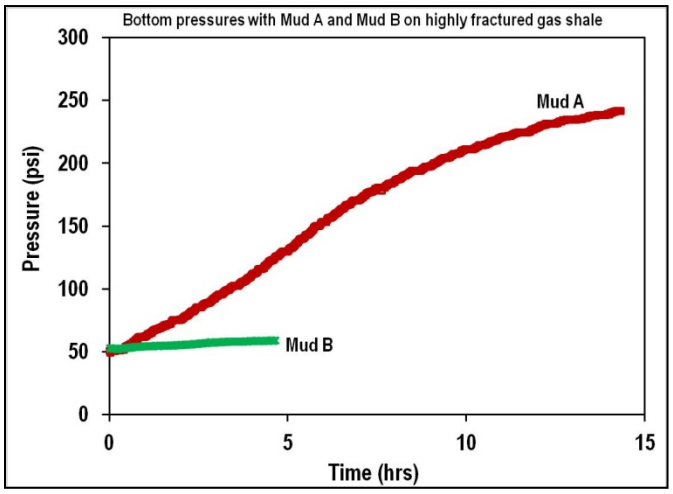

Fig. 13 – Pressures of Mud A and Mud B on highly fractured gas shale samples.

Tests on Slightly Fractured Gas Shale Samples

For the slightly fractured gas shale samples #3 and #4, the initial permeability with brine was on the order of 1,000 nD, as shown in Figure 14 and Figure 15. The Step 1 test with brine was able to be run using normal pressure penetration test, even through the bottom pressures (red data points) in the Step 1 showed a fast build up.

In Figure 14 and Figure 15, the bottom pressures with Mud A and C build up much slower than that with brines, respectively. Figure 16 plots bottom pressure with Mud A and C on slightly fractured gas shale samples. The bottom pressure built up slowly with Mud C, which contained nanoparticles.

As listed in Table 8, the permeability reduction was significant with both mud cases. Moreover, the permeability with Mud C containing nanoparticles was reduced more than Mud A as compared to their own initial permeability in Step 1. This again proves that nanoparticles can further plug shale pores and cracks, and reduce water invasion and maintain shale stability.

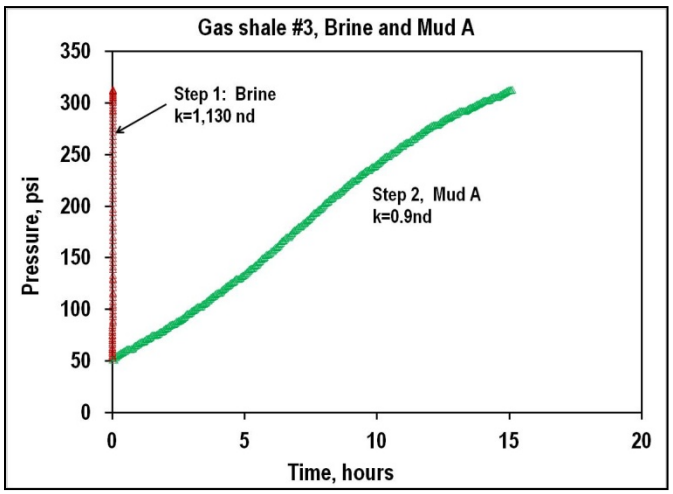

Fig. 14 – Pressure buildup of brine and Mud A on sample #3.

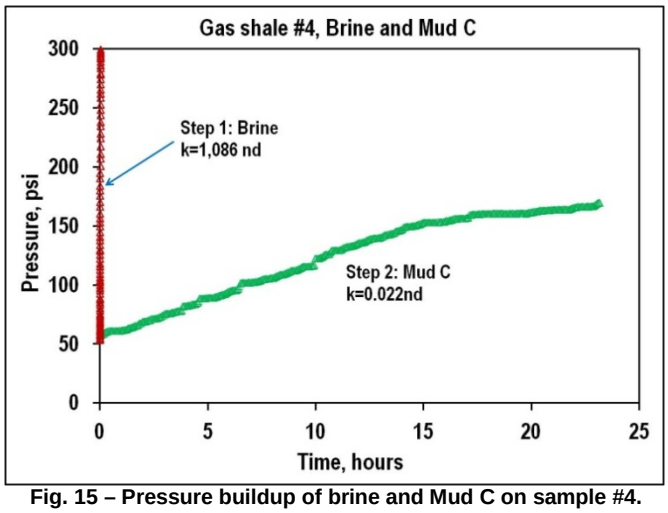

Fig. 15 – Pressure buildup of brine and Mud C on sample #4.

Table 8 – Permeability Reduction on Slightly Fractured Gas Shale Samples

Test Fluid	Brine Permeability (nD)	Mud Permeability (nD)	Permeability Reduction (%)
Mud A	1,130	0.9	100
Mud C	1,086	0.022	100

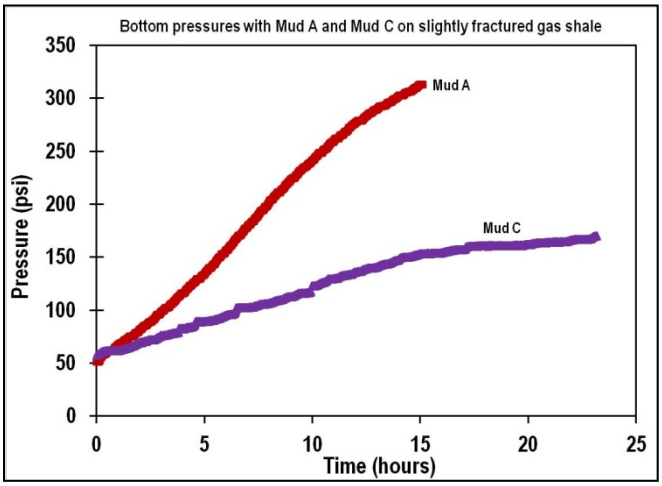

Fig. 16 – Pressures of Mud A and Mud C on slightly fractured gas shale samples.

Test with Multi-Fluids on Highly Fractured Gas Shale

A 4-step test was run on another gas shale sample #5 with brine, pure nanoparticle dispersion, Mud C and then Mud B respectively. The bottom pressure buildup and the corresponding permeability are shown in Figure 17 and Table 9.

Since gas shale sample #5 is highly fractured, a Darcy's flow test with brine (Step 1) was performed for the initial shale permeability with brine. Then another Darcy's flow test with pure nanoparticle dispersion (Step 2) was run to verify if pure nanoparticle dispersion could plug the cracks.

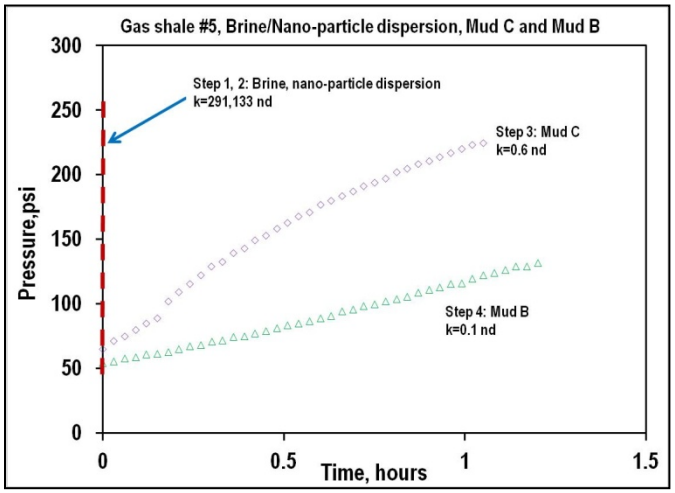

Fig. 17 – Pressure buildup of brine (Step 1), nanoparticle dispersion (Step 2), Mud C (Step 3) and Mud B (Step 4) on highly fractured gas shale sample (#5).

Pressure buildup and permeability in Step 2 were the same as that in Step 1. Pure nanoparticle dispersion alone could not plug the cracks in this highly fractured sample.

Then normal pressure penetration tests with Mud C (Step 3) and Mud B (Step 4) were run, respectively, on sample #5. The bottom pressures are shown in Figure 17, and permeability in Steps 3 and 4 are listed in Table 9. The permeability was reduced from 291,133 nD with brine and pure nanoparticle dispersion (Step 1 and Step 2) dramatically down to 0.6 nD with Mud C (Step 3) and further down to 0.1 nD with Mud B (Step 4). That proves that micro-cracks in this sample were effectively plugged with drilling fluid loss control agents and nanoparticles. The higher nanoparticle concentrations resulted in a better physical plugging to reduce water invasion into shale. Therefore, it confirms that nano-particles do behave as an effective physical inhibitor for this shale.

Table 9 – Permeability Reduction on Highly Fractured Gas Shale Sample #5

Test Fluid	Brine Permeability (nD)	Permeability Reduction (%)
Brine	291,133	n/a
Nano-particle dispersion	291,133	0
Mud C	0.6	100
Mud B	0.1	100(83*)
*: compared to permeability with Mud C		

Conclusions

Based on the above tests and analyses, the following conclusions are drawn.

- Water invasion into shale can be reduced or completely shutoff by physically plugging cracks and shale pores with an appropriately designed water-based drilling fluid containing suitable nanoparticles. The physical plugging is durable and sustainable. As a result, the shale becomes well inhibited.
- Nanoparticles alone can effectively plug pores in shale without microcracks, but alone cannot plug the micro-cracks. Combination of properly formulated mud and nano-particles of appropriate size and concentration is the key to prevent water invasion into shale samples with or without microcracks.

Acknowledgments

Authors thank Katherine Price-Hoelscher and George McMennamy for nanoparticle TEM photo and shale mineralogy.

Nomenclature

k	= *permeability of the shale*
t	= *test time*
A	= *cross-section area of shale sample*
C	= *compressibility of fluid in bottom reservoir*
L	= *thickness of shale sample*
M	= *fluid filtration viscosity*
$P0$	= *initial fluid (pore) pressure in shale sample*
$P2, P3$	= *top driving pressures above shale sample, flow-in and flow-out, respectively*
$P1$	= *bottom pressure in reservoir*
V	= *bottom reservoir volume*

References

1. Sandrea, R.: "Global Natural Gas Reserves – A Heuristic Viewpoint," *Middle East Economic Survey*, Vol. XLIX (March 2006).
2. Guo, Q., Ji, L., Rajabov, V., Friedheim, J., Portella, C. and Wu, R.: "Shale Gas Drilling Experience and Lessons Learned from Eagle Ford." SPE 155542, SPE Americas Unconventional Resources Conference, Pittsburgh, Pennsylvania, 5–7 June 2012.
3. Riley, M., Stamatakis, E., Young, S., Price-Hoelscher, K and De Stefano, G.: "Drilling Unconventional Shales with Innovative Water-Based Mud – Part II: Mud Formulations and Performance" AADE-12-FTCE-52, AADE Fluids Technical Conference, Houston 10-11 April 2012.
4. Al-Bazali, T.M., Zhang, J., Chenevert, M.E., and Sharma, M.M. "Factors Controlling the Membrane Efficiency of Shales When Interacting with Water-Based and Oil-Based Muds." SPE 100735, SPE International Oil & Gas Conference and Exhibition in China, Beijing, 5-7 December 2006.
5. van Oort, E.: "A Novel Technique for the Investigation of Drilling Fluids Induced Borehole Instability." SPE 28064, SPE/ISRM Rock Mechanics in Petroleum Engineering Conference, Delft, The Netherland, 29-31 August 1994.